Science of the Total Environment 872 (2023) 161997

Contents lists available at ScienceDirect

Science of the Total Environment

journal homepage: www.elsevier.com/locate/scitotenv

Evaluating changes in radionuclide concentrations and groundwater levels before and after the cooling pond drawdown in the Chornobyl Nuclear Power Plant vicinity

Hikaru Sato [a,*], Maksym Gusyev [b], Dmytro Veremenko [c], Gennady Laptev [d], Naoaki Shibasaki [e], Yuichi Onda [f], Mark Zheleznyak [b], Serhii Kirieiev [c], Kenji Nanba [b]

[a] Faculty of Life and Environmental Sciences, University of Tsukuba, Ibaraki, Japan
[b] Institute of Environmental Radioactivity, Fukushima University, Fukushima, Japan
[c] State Specialized Enterprise Ecocentre, SAUEZM, Chornobyl, Ukraine
[d] Ukrainian Hydrometeorological Institute, Kyiv, Ukraine
[e] Faculty of Symbiotic Systems Science, Fukushima University, Fukushima, Japan
[f] Center for Research in Isotopes and Environmental Dynamics, University of Tsukuba, Ibaraki, Japan

HIGHLIGHTS

- The Chornobyl cooling pond drawdown in 2014 changes the radionuclides' transport.
- Average groundwater levels declined from 0.5 m to 3.9 m at 65 % of shallow wells.
- ^{90}Sr increased at 21 % of shallow wells while ^{137}Cs did not.
- The ^{90}Sr concentration in the Pripyat Floodplain water increases.
- The ^{90}Sr contribution to the Pripyat River before and after the CP drawdown did not change significantly.

GRAPHICAL ABSTRACT

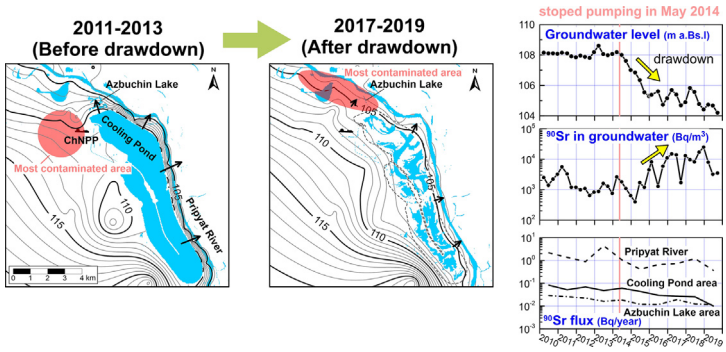

ARTICLE INFO

Editor: Christian Herrera

Keywords:
Surface water
Groundwater
Caesium-137
Strontium-90
Cooling pond drawdown
Chornobyl Nuclear Power Plant

ABSTRACT

In the vicinity of the Chornobyl Nuclear Power Plant (ChNPP), the cooling pond (CP) was an artificially maintained reservoir with water levels regulated to 7 m above the Pripyat River until May 2014, when its pumps stopped operating, resulting in a natural drawdown. To investigate the surface-groundwater system before and after the drawdown, we evaluated the spatial and temporal changes in ^{90}Sr and ^{137}Cs radionuclide concentrations and groundwater levels in the shallow unconfined aquifer near the ChNPP from 2010 to 2019. Additionally, we compared water levels and ^{90}Sr concentrations in Azbuchin Lake, wetlands inside the CP, and the Pripyat River. Using three-year averages before (2011 – 2013) and after (2017–2019) the drawdown period, we found that ^{90}Sr concentrations significantly increased up to 10^2 kBq/m^3 in the Pripyat River floodplain, north of ChNPP, exceeding the WHO drinking water guideline of 10 kBq/m^3. In contrast ^{137}Cs concentrations ranged consistently between 10 and 100 Bq/m^3. The groundwater levels decreased over 50 cm at approximately 65 % of shallow monitoring wells and up to 6 m near the CP. The ^{90}Sr concentration increases in some wells at the Pripyat River floodplain were associated with decreased dilution rates from the CP due to the reduced CP leakage, causing changes in groundwater flow direction and decreases in groundwater velocity. From the new finding of this study that the drawdown increased ^{90}Sr concentrations near the floodplain, we

Abbreviations: ChEZ, Chornobyl Exclusion Zone; ChNPP, Chornobyl Nuclear Power Plant; CP, cooling pond; RWDS, radioactive waste disposal site; RWTSP, radioactive waste temporary storage sites.

* Corresponding author at: Faculty of Life and Environmental Sciences, University of Tsukuba, 1-1-1 Tennodai, Tsukuba, Ibaraki 305-8572, Japan.
E-mail address: sato.hikaru.gf@alumni.tsukuba.ac.jp (H. Sato).

http://dx.doi.org/10.1016/j.scitotenv.2023.161997
Received 29 November 2022; Received in revised form 20 January 2023; Accepted 30 January 2023
Available online 02 February 2023

estimated the ^{90}Sr flux and contribution to the Pripyat River and the ^{90}Sr contribution did not change significantly after the drawdown. However, radionuclides may accumulate more at the floodplain in the future; therefore, additional monitoring is required to verify ^{90}Sr transport from areas of elevated concentrations and its impact on groundwater in the aquifer.

1. Introduction

Radioactive materials remaining in the environment due to nuclear accidents and waste contaminate the surrounding environment over the long term. The Chornobyl and Fukushima Daiichi nuclear power plant accidents released radioactive plumes into the atmosphere and contaminated water bodies, soils, and vegetation near their sites with radioactive fallout (Beresford et al., 2016; Onda et al., 2020). Additionally, nuclear fuel processing facilities and landfills for highly radioactive waste related to the decommissioning of nuclear facilities also contaminate the surrounding soil (Fredrickson et al., 2004; Tyler, 2020). Radioactive materials migrate from these contaminated soils into groundwater and are discharged into rivers and seepage areas via groundwater flow (Bixio et al., 2002; Dai et al., 2002; Slater et al., 2010; Zachara et al., 2013). Concerns remain that the discharge of highly contaminated groundwater may adversely affect drinking water and the surrounding flora and fauna (Lerebours et al., 2018; Mappes et al., 2019).

In April 1986, the Chornobyl Nuclear Power Plant (ChNPP) accident released a large amount of nuclear fuel particles, including ^{137}Cs and ^{90}Sr, which were deposited on the ground near the ChNPP site. Access to these areas was limited via the 30-km Chornobyl Exclusion Zone (ChEZ), and radionuclide monitoring was performed from the ChEZ to the downstream area of Pripyat River to avoid radionuclide migration downstream to Kyiv. In the ChEZ, ^{137}Cs and ^{90}Sr concentrations as of 1997 reached a high of more than 4000 kBq/m^2 near the reactor building, and the highly concentrated area expanded to the west and northwest from the ChNPP (Kashparov et al., 2018). To address this issue, contaminated topsoil, vegetation, and construction debris were buried in trenches near the ChNPP during clean-up activities in 1987–1988 (International Atomic Energy Agency [IAEA], 2006). In the ChNPP area, 800 trenches are subdivided into "sectors," and these sectors are a potential source of radionuclide migration to groundwater (Dewiere et al., 2004; Roux et al., 2014). Among the radioactive materials in the soil and trenches, ^{90}Sr poses the greatest threat to groundwater contamination because of its high mobility and susceptibility to hydrogeological effects (Bugai et al., 1997). For example, the solid/liquid distribution coefficient (Kd) of ^{90}Sr was the lowest (2–17 mL/g) in those of Cs and Pu (Bugai et al., 2020). Another potential source of radionuclide contamination in the ChNPP area is the cooling pond (CP), which was an artificial reservoir located on the floodplain used to cool the ChNPP reactors (Bugai et al., 1997, 2022).

The CP was heavily contaminated by the fallout from the ChNPP accident. The ^{90}Sr concentrations in the water increased for several years after the accident due to the breakdown of fuel particle but have been decreasing since 1990, stabilizing during 2000–2010 at 1–2 kBq/m^3 (IAEA, 2019; Nasvit, 2002). As an artificial reservoir, the CP water balance was maintained by a continuous inflow of water pumped from the Pripyat River, its outflows were evaporation, exfiltration seepage to drainage ditches, and leakage to groundwater through bottom sediments (Bugai et al., 1997; IAEA, 2019). The primary release pathway for ^{90}Sr and ^{137}Cs was seepage of contaminated water into drainage ditches and subsurface pathway leakage. Release from the cooling pond in 2010 contributed approximately 10 % of the total ^{90}Sr transport by the Pripyat River (Bugai and Skalskky, 2013; IAEA, 2019). In May 2014, the pumping was discontinued, initiating an uncontrolled drawdown of the CP and raising a major concern regarding the radionuclides in the CP bottom sediments that accumulated over the years after the drawdown (Bulgakov et al., 2009; IAEA, 2019). For example, the mobilization of contaminants from fuel particles in the newly exposed areas of the CP is associated with the change of pH due to the surface water decline (Bulgakov et al., 2009). In addition, leakage of water and radionuclides from the bottom of the CP influenced the groundwater flow regime and radionuclide concentrations on a large scale. Numerous previous studies have focused on interactions between the CP and nearby surface water features and radionuclide migration during CP operation. However, no studies have evaluated the changes in surface-groundwater interactions before and after the drawdown.

Downward migration of ^{90}Sr from the shallow trenches to groundwater in the Red Forest and ChNPP sites located 2.5 km southwest of the ChNPP was investigated by field and modeling studies (Bugai et al., 2002, 2007, 2012a, 2012b; Le Gal La Salle et al., 2012; Matoshko et al., 2004; Van et al., 2009, 2012; Onishi et al., 2007). According to Bugai et al. (2002), the ^{90}Sr migration velocity at the pilot site was extremely slow compared to the groundwater flow velocity. Prior to the drawdown, the ^{90}Sr transport to the Pripyat River was estimated using field data from tracer experiments at wells in the dike between the CP and Pripyat River (Bugai et al., 2005; Bugai and Skalskky, 2013, 2018). However, these studies analyzed data that were collected during CP operation, and only one study by Bugai et al. (2022) included data on post-operation groundwater levels and radionuclide concentrations, which found only five out of 73 wells with increasing ^{90}Sr concentrations by investigating long-term trends in annual radionuclide data and groundwater levels in wells in the unconfined and confined aquifers. Therefore, no evaluation exists of the surface-groundwater flow system and shallow unconfined aquifer before and after the CP drawdown, and an investigation of ^{90}Sr concentration changes and migration is needed in the vicinity of the CP and ChNPP sites. Furthermore, the flux of ^{90}Sr to the Pripyat river after the drawdown is important in clarifying the impact of the large-scale decline of groundwater level.

Thus, evaluating changes in the groundwater system and radionuclide concentrations associated with the large-scale drawdown in CP water level is important for long-term management near the CP and for predicting increases in radionuclide concentrations. This study evaluated changes in ^{90}Sr and ^{137}Cs concentrations and groundwater levels in wells in the shallow unconfined aquifer in the vicinity of ChNPP before and after the CP drawdown. We selected monitoring wells with monthly measurements from 2010 to 2019 and quantified spatial changes using a 3-year average of ^{90}Sr and ^{137}Cs concentrations before (2011–2013) and after drawdown (2017–2019). Temporal changes were evaluated using time-series data of monthly ^{90}Sr and ^{137}Cs concentrations, and observed groundwater levels were compared with the Pripyat River water levels near the CP. We re-examined seasonal changes in the groundwater levels to analyze changes in the behavior of the hydrological system and compared the groundwater transport of ^{90}Sr to the Pripyat River before and after the drawdown. We also compared the 3-year average ^{90}Sr concentrations in shallow groundwater with the CP surface water and Azbuchin Lake (Fig. 1) to understand the effects of large-scale environmental changes and provide important baseline data for the monitoring and sustainable management of environmental radioactivity and numerical radionuclide modeling.

2. Study area

2.1. Cooling pond

The CP was constructed southeast of the ChNPP in 1976 and enlarged in 1981, with a surface area of 22.9 km^2 and a water volume of 151 × 10^6 m^3 (IAEA, 2019) (Fig. 1). The water balance during operation was determined by the inflow of water pumped from the river, and the outflows consisted of evaporation, seepage into the north and south drainage channels, and

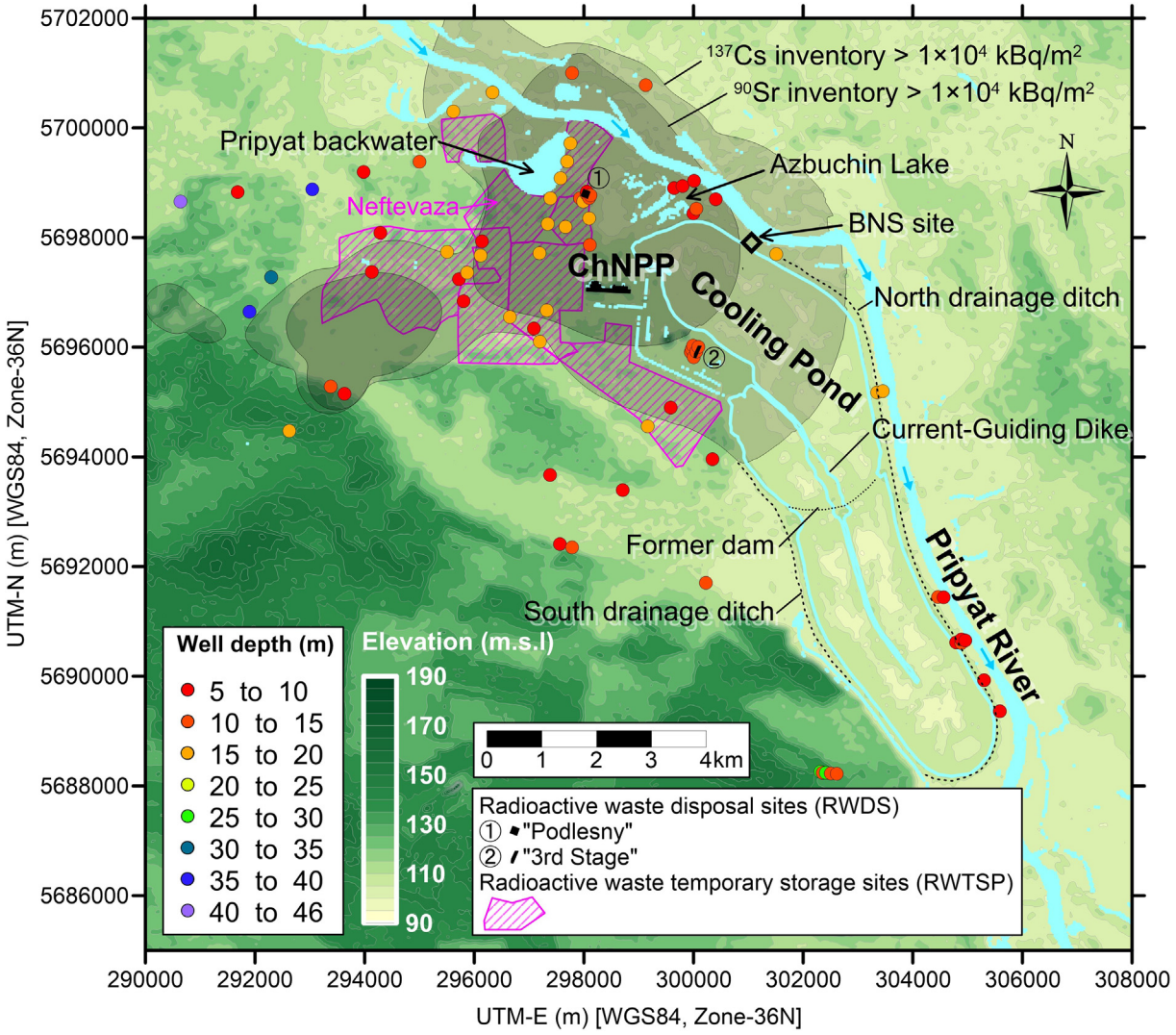

Fig. 1. Location of monitoring wells in the vicinity of the Chornobyl Nuclear Power Plant (ChNPP) with the colour-coded well depth. Surface water features as of August 13, 2013 are colored light blue and mapped using selected low cloud-cover Landsat8 C2L2 (QA_PIXEL) images downloaded from the United States Geological Survey (USGS) EarthExplorer (https://earthexplorer.usgs.gov/). Surface water features are shown above the terrain elevation. The cooling pond (CP) is shown by blue line and the area inside of the CP is colored according to its bathymetry based on Buckley et al. (2002). The shaded area indicates the spatial distribution of ^{137}Cs and ^{90}Sr concentrations exceeding 1 × 10^4 kBq/m^2 as of 1986, which were estimated by inverse estimation using half-life based on the database of Kashparov et al. (2018). The black polygon and pink polygon with slant stripe indicate the radioactive waste disposal site (RWDS) and radioactive waste temporary storage sites (RWTSP), respectively. (For interpretation of the references to colour in this figure legend, the reader is referred to the web version of this article.)

leakage to the underlying aquifer (Fig. 2a, Bugai et al., 1997). Water was pumped from Pripyat River at the BNS site north of the CP (Fig. 1). The water level during the operation was set at approximately 111 m above Baltic Sea level (a.Bs.l.), which is 6–7 m higher than that of the Pripyat River. An investigation of the bathymetry in 1999–2001 (Buckley et al., 2002) reported a lowest elevation of 94 m a.Bs.l. with deeper sites in the southern portions of the CP. The area below 7.0 m in depth accounts for 16.81 km^2 of the CP, which means that 75 % of the ground is exposed when the water level is approximately 104 m a.Bs.l. After decommission, the water level declined by 6.2 m from May 2014 at 110.8 m to December 2021 at 104.6 m a.Bs.l. The CP drawdown was significant at 1.8 m/y from May 2014 to 2016 and subsequently decreased to 0.4 m/y from 2017 to 2019 (Kanivets et al., 2020). The CP reservoir was divided into three areas after 2016 when the water level reached 106 m a.Bs.l. The northern and southern areas were separated by the former dam installed in the 1st stage of the ChNPP, and the northern area was further divided into east and west by the Current-Guiding Dike (Fig. 1 IAEA, 2019). The water level subsequently decreased below the bottom of the northern and southern drainage channels, stopping the seepage and drainage flow. In the current water balance, the inflow is only precipitation, and the outflows are evapotranspiration and leakage into the subsurface (Fig. 2b IAEA, 2019).

2.2. Topography and hydrogeology around the ChNPP site

The terrain below 120 m a.s.l. around the CP consists mainly of alluvial sandy sediments (Matoshko et al., 2004). The western side is elevated by terraces, with elevations ranging from approximately 130 to 190 m (Fig. 1). Numerous lakes and marshes of various sizes exist in the floodplain of the Pripyat River, including the Pripyat backwater and Azbuchin Lakes, which are located 2.5 km and 0.8 km west of the CP, respectively. During pumping, the water level in the CP was higher than that in Azbuchin Lake and the Pripyat River. This caused CP water to feed into both water bodies.

The unconfined aquifer near the ChNPP consists of Holocene, Pleistocene, and Pliocene aeolian and alluvial sandy sediments (Matoshko et al., 2004). The Chornobyl site is located on the first terrace above the floodplain on the right bank of the Pripyat River, where the unconfined aquifer

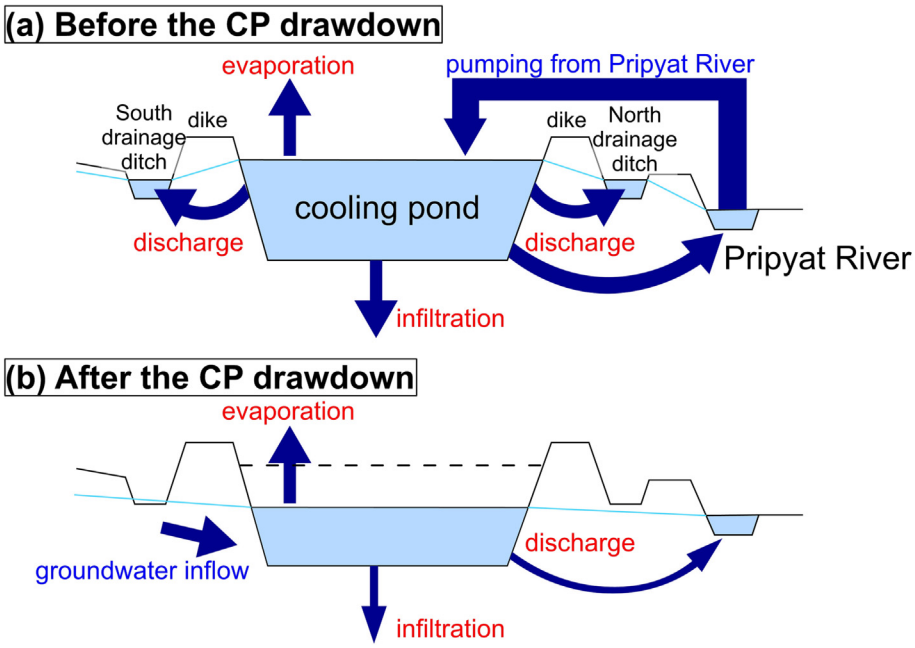

Fig. 2. Water balance of the CP before and after the drawdown. a: the water balance of the CP before the drawdown. b: the water balance of the CP after the drawdown. This figure was made based on Bugai et al. (1997).

is approximately 30 m thick. In the floodplain, where the CP site is located, the unconfined aquifer is 18–20 m thick. The hydraulic conductivity of the aquifer was estimated to be 5–25 m/day based on pumping tests (Bugai et al., 1997). Underlying the Pleistocene or Pliocene sandy sediments are Eocene marine carbonate silts and marls approximately 10–20 m thick, forming a low permeable layer.

2.3. Radionuclide waste storage site vicinity of the ChNPP

Within a 10 km radius of the ChNPP, there are two radioactive waste disposal sites (RWDS) (Fig. 1). The "Podlesny" RWDS is located north of the ChNPP, between the Pripyat backwater and CP (Fig. 1). This repository was intended for the disposal of high-level waste with dose rates of 0.05 to 2.5 Gy/h or higher at 10 cm below the surface. Approximately 11,000 m^3 of waste, mainly building materials, metal fragments, sand, concrete, and wood, is contained in two vaults therein and covered with concrete (IAEA, 2006). The total radioactivity of the waste was estimated to be 2600 TBq in 1990 (IAEA, 2006). The "3rd Stage" RWDS consists of an underground concrete vault located on a man-made "islet" formed by the CP and spillway (Fig. 1; IAEA, 2019). This facility contains mainly sand, concrete, metal, construction material, and brick wastes at low and intermediate levels with dose rates of up to 0.01 Gy/h at 10 cm from the surface of the waste container (IAEA, 2006). More than 26,200 m^3 of solid waste, with a total radioactivity of 4×10^{14} Bq, was stored in containers therein and covered with sand and clay. The groundwater table is high in this area, and the facility was flooded to 0.5–0.7 m above the bottom before the CP drawdown (IAEA, 2006).

Unlike the RWDS, radioactive waste temporary storage sites (RWTSP) near the ChNPP did not use storage containers (IAEA, 2006). This is where low-level radioactive waste, including vegetation, soil, and debris, from the 1987–1988 clean-up are stored (IAEA, 2006). The waste is stored in trenches or pits 2.0–2.5 m deep and 6–7 m high (Ledenev et al., 1995), with a total volume estimated at approximately 1.5×10^6 m^3 with a total radioactivity of 3.5×10^{14} Bq in 2015 (Molitor et al., 2017). There has been no work to waterproof the bottom of the trench or pit, or to install screens to prevent infiltration. The RWTSP is the greatest groundwater contamination concern and the "Neftevaza" RWTSP, located along the shore of Pripyat backwater where 39 trenches containing radioactive waste in the floodplain area are flooded with groundwater (Ledenev et al., 1995). Additionally, several RWTSP are located in inappropriate hydrogeological locations (IAEA, 2019).

2.4. Monitoring wells for groundwater level and radionuclides near the ChNPP

The State Specialized Enterprise Ecocentre measured groundwater levels during 1986–2019 and collected groundwater samples during 1993–2019 at 148 monitoring wells, which are in the unconfined aquifer. Well depths are 2–40 m, with an average of 16 m, and 50 % of all wells are shallower than 10 m deep. Areas with high concentrations were sampled monthly, whereas other areas were sampled once every three months. Groundwater near the ChNPP was managed by the State Specialized Enterprise Ecocentre located within the ChEZ.

3. Methods

3.1. Sampling of surface water and groundwater

In the ChEZ, gauging sites with water level bars were established at all surface water ponds and streams, and water sampling was conducted using polyethylene storage tanks, a water sampling bucket, and a glass bathometer bottle. The Pripyat River levels were measured at the BNS site in the northern part of the CP (Fig. 1) and in the Chornobyl City about 17 km downstream from the BNS site. River water samples were collected at the Pripyat River at Chornobyl City site using either a boat or a 1 L glass bathometer simultaneously at two river depths, as well as by measuring river velocity. The two river depths were approximately 0.2 m below the water surface and 0.8 m above the river bottom for at least 10 locations across the river width to obtain an average for all samples. Low- and non-flowing lakes, ponds, and CP were sampled at the maximum distance from the bank. The groundwater level was measured before sampling using a manual water level gauge and well purging. Following initial pumping to obtain clear groundwater, groundwater was sampled using the pump and promptly stored in polyethylene containers. Prior to surface and groundwater sampling, the collection equipment was thoroughly rinsed with sampled water at each site, which was held in 19 L and 1 L storage tanks for ^{137}Cs and ^{90}Sr analyses, respectively. The analytical procedures for concentrating large volume of water samples for radiometric

measurements such as using exchange resins for ^{137}Cs and radiochemical concentration for ^{90}Sr are described in detail by Bugai et al. (2022).

The ^{137}Cs was measured via gamma spectrometry 919 Spectrum Master 4-channel analyzer (Ortec, USA) with PGT (Princeton Gamma-Tech) detectors (Canberra) with an efficiency of 25–50 % and a Nokia LP-4900B 2-channel detector (Nokia, Japan) for X-ray gamma spectrometry with detectors (Canberra; Ortec) with 10 % efficiency. The radionuclide ^{90}Sr was measured using an NRR-610 low-level alpha-beta radiometer (Tesla, USA), which can hold up to 55 samples simultaneously, and an SEB-01–150 beta-spectrometer (Atom Komplex Prylad, Ukraine), which consists of an intelligent scintillation detection unit at 150 mm, passive low-background protection, and AKWin software (Atom Komplex Prylad, Ukraine).

3.2. Water level and radionuclide concentrations used for analysis

Contour maps and bubble plots were prepared to determine the distributions of water levels and radionuclide concentrations, respectively. The measurement frequency of the groundwater level and radionuclide concentrations varied depending on the monitoring well locations, which were sampled more frequently near the ChNPP (Supplementary, Table. S1, S3). Therefore, long-term observation data for the groundwater levels were correlated with water levels in the Pripyat River or nearby groundwater to interpolate the values for unmeasured periods. The groundwater levels for each period were determined using this method. The surface water levels of the Pripyat River measured at the BNS gauge (Fig. 1) and CP were utilized to define groundwater gradients as groundwater flow discharge boundaries. Using these data, a contour map of the groundwater level was created using the kriging method. However, radionuclide concentrations during unmeasured periods could not be estimated by using surrounding radionuclide data due to irregular variations. Therefore, distribution maps were prepared based on 3-year averages of the concentrations. The raw data and statistical analyses was shown in Supplementary Table S1 for ^{90}Sr and Table S3 for ^{137}Cs. ^{90}Sr data depict the variability in the data at each well before and after the CP drawdown and confirm the validity of most of the well data that we used for analysis; however, some data have large standard deviations. ^{137}Cs data was sampled less frequently about half of ^{90}Sr and showed greater variability than ^{90}Sr. In addition, multiple depth-specific strainers were installed at in some locations, and the shallowest wells were used for distribution maps of groundwater levels and radioactive concentrations (Fig. 1). Hence, 88 % of all monitoring wells for analysis were shallower than 20 m.

Six characteristic sites near the CP were selected to measure the groundwater level and radionuclide concentration trends for each well (Table 1). Wells 3A, 2A, 1A, and PK-14 1B, 2B, and 3B were installed north of the CP in Pripyat River floodplain, which contains small ponds. Wells 2/1 and 168 were installed west of the CP near the ChNPP. Wells 193 and PK-127 were installed in the southwest and southeast, respectively. The shallowest well at the 168 location (168/Q1) stopped observations in October 2014 after the CP decommission because no water remained in the well. Therefore, 168/Q2 was used to create the distribution maps.

3.3. ^{90}Sr transport analysis

The ^{90}Sr flux (TBq/y) to the Pripyat River was calculated using the following equation, which was described by Bugai and Skalskky (2013):

$$A_{sub}(t) = Q_{sub} \times C_{ave}(t - \Delta t) \quad (1)$$

where $A_{sub}(t)$ (Bq) is the ^{90}Sr flux through the subsurface, Q_{sub} (m^3/d) is the groundwater discharge, C_{ave} (Bq/m^3) is the yearly average ^{90}Sr concentration in wells, and t (d) and Δt (d) are the time of measurement and time required for ^{90}Sr migration from the well to the Pripyat River, respectively. Q_{sub} is calculated as

$$Q_{sub} = V_{real} \times n \times L \times h \quad (2)$$

Table 1
Specifications of monitoring wells.

No.	Well ID	Coordinate (degree)		Wellhead elevation (m a.s.l.)	Well Depth (m)	Screen inner diameter (mm)	Screen interval (m below ground)	
		Longitude	Latitude				From	to
1	1A	30.12437	51.40720	106.42	9.15	89	6.7	8.2
2	2A	30.12146	51.40626	110.43	9.88	89	7.4	8.9
3	3A	30.11920	51.40592	107.72	6.18	89	3.6	5.1
4	PK-14 1B	30.12457	51.40189	108.43	9.2	89	7.1	8.6
5	PK-14 2B	30.12529	51.40266	108.10	10.7	89	8.7	9.7
6	PK-14 3B	30.13028	51.40432	106.30	7.0	89	5.8	6.8
7	2/1	30.08568	51.37986	113.97	15.0	122	2.1	14.1
8	168/Q1	30.09771	51.39603	115.22	12.9	114	7.3	11.3
9	168/Q2			115.26	19.2	110	16.8	18.2
10	168/Q3			115.35	30.0	110	27.3	28.8
11	193/Q1	30.13204	51.36175	113.29	9.0	114	4	8
12	193/Q2			113.23	19.6	110	17.2	18.6
13	193/Q3			113.33	31.0	110	26.5	28
14	PK-127 127/1	30.20979	51.32231	105.85	18.8	89	17	18
15	PK-127 127/2			105.80	16.8	89	15	16
16	PK-127 127/3			105.80	6.8	89	5	6

where V_{real} (m/d) is the actual velocity, n (unitless) is the porosity, L (m) is the length of the floodplain between the CP and Pripyat River used for the groundwater filtration calculation, and h (m) is the aquifer thickness or water table depth in the unconfined aquifer. V_{real} was estimated by Bugai et al. (2005) as follows, as the ^{90}Sr migration velocity, V_{Sr} (m/d), in the groundwater:

$$V_{Sr} = \frac{V_{real}}{R} \quad (3)$$

$$R = 1 + \frac{\rho K_d}{n} \quad (4)$$

where R (unitless) is the ^{90}Sr retardation factor estimated from the ^{90}Sr sorption distribution coefficient (Kd [m^3/g]), soil density (ρ[g/m^3]), and porosity. The Δt was estimated from the distance (D [m]) and the ^{90}Sr migration velocity (V_{Sr}), as follows:

$$\Delta t = D/V_{Sr} \quad (5)$$

^{90}Sr concentrations and groundwater levels of wells PK-14 3 B, PK-32 64, PK-64 92/2, and PK-113 151 3 k were used for flux calculations, similar to Bugai and Skalskky (2013). In this study, ^{90}Sr transport was also calculated for well 1A, located near Azbuchin Lake, which showed high ^{90}Sr concentrations in the lake water. Bugai et al. (2005) and Bugai and Skalskky (2013, 2018) used the groundwater velocities measured by single-hole tracer dilution tests (Bugai et al., 2005) as V_{real} in the aquifer. In this study, the Darcy velocity using the hydraulic gradient between the well and the river was used as $V_{real} \times n$, because the velocities were not obtained at the wells and changed after the CP drawdown. The well information and parameters used for the ^{90}Sr transport calculation are listed in Supplementary Table S5. Our calculations used representative wells near the river and assumed that the concentrations in these wells were representative of the concentrations throughout the unconfined aquifer. Therefore, the results potentially overestimated the risk considerations.

4. Results

4.1. ^{90}Sr concentrations change in monitoring wells

The average ^{90}Sr concentrations in the monthly wellbore samples during 2011–2013 and 2017–2019 are shown in Fig. 3a and b, respectively.

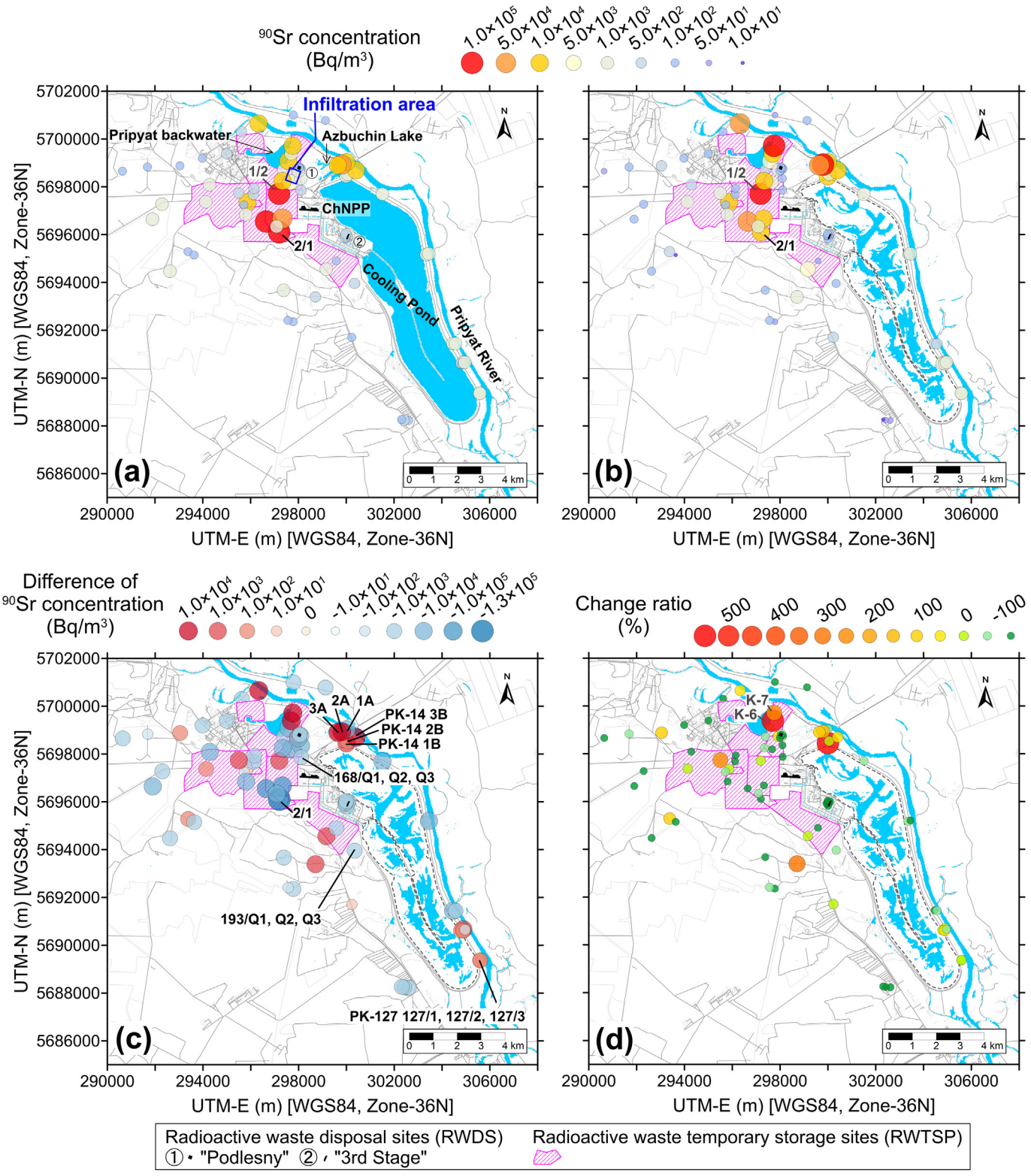

Fig. 3. Average ^{90}Sr concentrations in monthly wellbore samples during (a) 2011–2013 and (b) 2017–2019, (c) the difference between them, and (d) the change ratio. The size and colour of the bubbles indicate the magnitude of the concentration or ratio. Surface water features are shown by blue areas. The water areas are colored light blue (a: as of August 13, 2013; b, c and d: as of May 19, 2019) and were mapped using selected low cloud-cover Landsat8 C2L2 (QA_PIXEL) images downloaded from the United States Geological Survey (USGS) EarthExplorer (https://earthexplorer.usgs.gov/). The infiltration area of the ChNPP wastewater treatment plant is indicated by blue polygon at north of the ChNPP. The black polygon and pink polygon with slant stripe indicate the radioactive waste disposal site (RWDS) and radioactive waste temporary storage sites (RWTSP), respectively. (For interpretation of the references to colour in this figure legend, the reader is referred to the web version of this article.)

The difference between them is shown in Fig. 3c, and the rate of change is shown in Fig. 3d. The ^{90}Sr concentration data used for Fig. 3 are presented in Supplementary Table S1.

Prior to the CP drawdown (2011–2013), the average concentration of ^{90}Sr was highest (1.5×10^5 Bq/m^3) at monitoring well 2/1, located southwest of the ChNPP (Fig. 3a). Monitoring well 1/2, located 1.6 km north of well 2/1, had the second highest concentration, at 1.2×10^5 Bq/m^3 (Fig. 3a). Additionally, the average ^{90}Sr concentrations in groundwater show an order of magnitude difference from the southern area at the ChNPP to the northern area near the Pripyat River (Fig. 3a). These distributions are consistent with the estimated surface deposition in 1986 (Fig. 1), indicating that the high-concentration distribution area did not extend to the west or east. In addition, an infiltration area of the ChNPP wastewater treatment plant was present north of the ChNPP, and the average ^{90}Sr concentrations in this area were low (Fig. 3a). Moreover, concentrations at the Pripyat River ranged from 32 to 590 Bq/m^3. The average ^{90}Sr concentrations in the wells between the CP and Pripyat River were two orders of magnitude smaller than those southwest of ChNPP and ranged from 1.0×10^2 to 5.0×10^3 Bq/m^3. The concentrations on the floodplain between the CP and Pripyat River were approximately an order of magnitude higher than those upstream of the CP.

Fig. 3b shows the average ^{90}Sr concentrations during 2017–2019, when the highest concentration was 1.4×10^4 Bq/m^3 at well 2A. In Fig. 3b, well 1/2 had the second highest concentration of 1.2×10^4 Bq/m^3. Moreover, the average ^{90}Sr concentrations in groundwater in the north near the Pripyat River were an order of magnitude higher than those in the southwest (Fig. 3b). For the monitoring wells near Azbuchin Lake, the average ^{90}Sr concentrations were high, whereas the average ^{90}Sr concentrations near the infiltration area north of the ChNPP were low (Fig. 3b). Additionally, the Pripyat River concentrations ranged from 24 to 260 Bq/m^3. The concentrations on the dike between the CP and Pripyat River were approximately an order of magnitude higher than those in the southwestern of the CP.

Fig. 3c shows the difference between the 3-year averages of ^{90}Sr concentrations before and after the CP drawdown; they ranged between -1.3×10^5 Bq/m^3 at well 2/1 to 8.5×10^4 Bq/m^3 at well 2A. Increases in ^{90}Sr concentrations above 1.0×10^4 Bq/m^3 were found near the small lakes near the Pripyat River. Using data on the unconfined aquifer from 148 monitoring wells, the average ^{90}Sr concentrations increased in 31 wells, and some nested wells showed increases in both shallower and deeper screens, such as wells 2A and 2 near Azbuchin Lake. Specifically, the average ^{90}Sr concentration increased by 8.5×10^4 Bq/m^3, from $5.2 \pm 1.0 \times 10^4$ Bq/m^3 to $13.8 \pm 5.3 \times 10^4$ Bq/m^3, at well 2A (9.88 m deep) and 1.5×10^4 Bq/m^3, from $1.6 \pm 0.4 \times 10^4$ Bq/m^3 to $3.1 \pm 0.2 \times 10^4$ Bq/m^3, at well 2 (14.29 m deep). However, well 1/2 showed a small change of 2.3×10^3 Bq/m^3; the average ^{90}Sr concentrations remained high before and after the drawdown. Thus, this small change at well 1/2 led to the minor change ratio shown in Fig. 3d.

Fig. 3d shows the rate of change in the average concentrations before and after the CP drawdown to identify new "hot spots with increasing ^{90}Sr concentrations. As shown in Fig. 3d, the average ^{90}Sr concentration in groundwater decreased southwest of the ChNPP, whereas the concentrations increased significantly on the north side, near the Pripyat River. In particular, the figure indicates that the two hotspots were near the Pripyat River, which had up to 600 % increased ^{90}Sr concentrations in water. Hence other than these hotspots most of the area showed decreased ^{90}Sr concentrations. Moreover, most of the wells near the RWDS, where radioactive waste was stored in containers, showed decreasing concentration trends.

The same analysis was performed for ^{137}Cs as for ^{90}Sr (Supplementary Table S3, Fig. S1). However, evaluating the changes in ^{137}Cs was more difficult that for ^{90}Sr, because the ^{137}Cs data had larger standard deviations and fewer measurements than those of ^{90}Sr. When only shallow wells are used for analyzing as shown in Fig. S1, more than 90 % of the ^{137}Cs concentrations were lower than 10^2 Bq/m^3, with no significant difference between before and after the drawdown compared to ^{90}Sr concentrations (Supplementary Fig. S1 a–c). However, total three wells showed increase the change rate significantly greater than 300 % in the unconfined aquifer. It can be seen at well 4H at the Podlesny RWDS, well 13 at the 3rd Stage RWDS, and well 171/1 located inside the RWTSP (Supplementary Table S3 and Fig. S1 (d)). Other 5 lower wells except for well 201 also increased the change ratio and they are located inside the RWTSP near the well 171/1. The wells with significantly increase in the change ratio are located in the vicinity of the radioactive waste facilities. ^{137}Cs in well 201 on the left bank of the Pripyat River also increased, however the relationship to the radionuclide waste site is nothing.

4.2. Monthly time-series data of groundwater levels and ^{90}Sr and ^{137}Cs concentrations

Figs. 4 and 5 show the time-series data of monthly precipitation, groundwater levels, and concentrations at representative wells with increasing and decreasing average ^{90}Sr concentrations. The locations of these 10 wells are shown in Fig. 3c and their 16 screens are listed in Table 1. At 168 and 193Q, three monitoring wells were nested with a screen at different depths in each well. In Figs. 4 and 5, the three panels show the observed time-series data from 2010 to 2019 for each screen, and the vertical pink line shows the start of the CP drawdown. This panel setup allows us to compare the CP influence before and after the drawdown. In Fig. 4, monthly Pripyat River water levels measured at the BNS site after the drawdown were used for wells situated 1–1.5 km upstream of the BNS site (Fig. 4a and b), and monthly river water levels measured at the city of Chornobyl were used for the nested well situated 10 km downstream of the BNS site (Fig. 4c). In addition, the Azbuchin Lake data are shown in Fig. 4a with a focus on 2016–2019.

In the top panels of Fig. 4a–c, groundwater levels were affected by the water levels of the Pripyat River, which were highest during the snowmelt season from March to May and heavy rainfall events. Annual precipitation at the ChNPP from 1990 to 2019 was 612.6 ± 99.5 mm, the largest amount was 953.8 mm in 2012. The wet- (May to August) and dry- (January to April) season precipitation was 50–70 mm/month and 30–40 mm/month, respectively. The monthly precipitation exceeded 150 mm in July 2011, August 2012, May 2014, and October 2016. As shown in Fig. 4a, the groundwater levels at 3A, 2A, and 1A before the CP drawdown were approximately 104–107 m a.Bs.l. and fluctuated approximately 1–2 m with the Pripyat River levels. The groundwater levels declined by approximately 1–2 m after the CP drawdown and approached the level of the Pripyat River during flooding. The water levels in the wells near Azbuchin Lake were maintained at a higher level than that of the downstream groundwater levels before the CP drawdown. However, the groundwater and Azbuchin Lake levels were reversed during the rainy season after the CP drawdown.

As shown in Fig. 4b, wells PK-14 1B and 2B, located near the CP, showed no response to the fluctuations of the Pripyat River levels; in contrast well 3B, situated near the river, responded to the Pripyat River before the CP drawdown. The groundwater levels in these wells were approximately 107–108 m and 104–105 m, respectively with a difference of approximately 3 m. After the CP drawdown, the groundwater levels in both 1B and 2B declined to 105 m and responded to fluctuations in the Pripyat River. The groundwater levels of well 3B were similar to the level of Pripyat River, at approximately 104 m, indicating surface-groundwater connectivity. A similar pattern was also observed in nested well PK-127 (Fig. 4c), which was situated south of the CP. The groundwater levels, which were nearly constant at approximately 105 m, declined by 2 m after the CP was decommission and began to respond to the Pripyat River. The pattern of fluctuations in groundwater levels at wells 2/1, 168, and 193, which are located at a distance from the Pripyat River and shown in Fig. 5a, b, and c, respectively, remained the same after the CP drawdown, with a groundwater level drop of 1–2 m.

From the middle panels in Fig. 4, we identified increasing and consistent seasonal trends in ^{90}Sr concentrations after the CP drawdown. As shown in Fig. 4a, ^{90}Sr concentrations in wells 3A, 2A, and 1A were between 10^4 and 10^5 Bq/m^3 during 2010–2013; after the drawdown, values at 3A

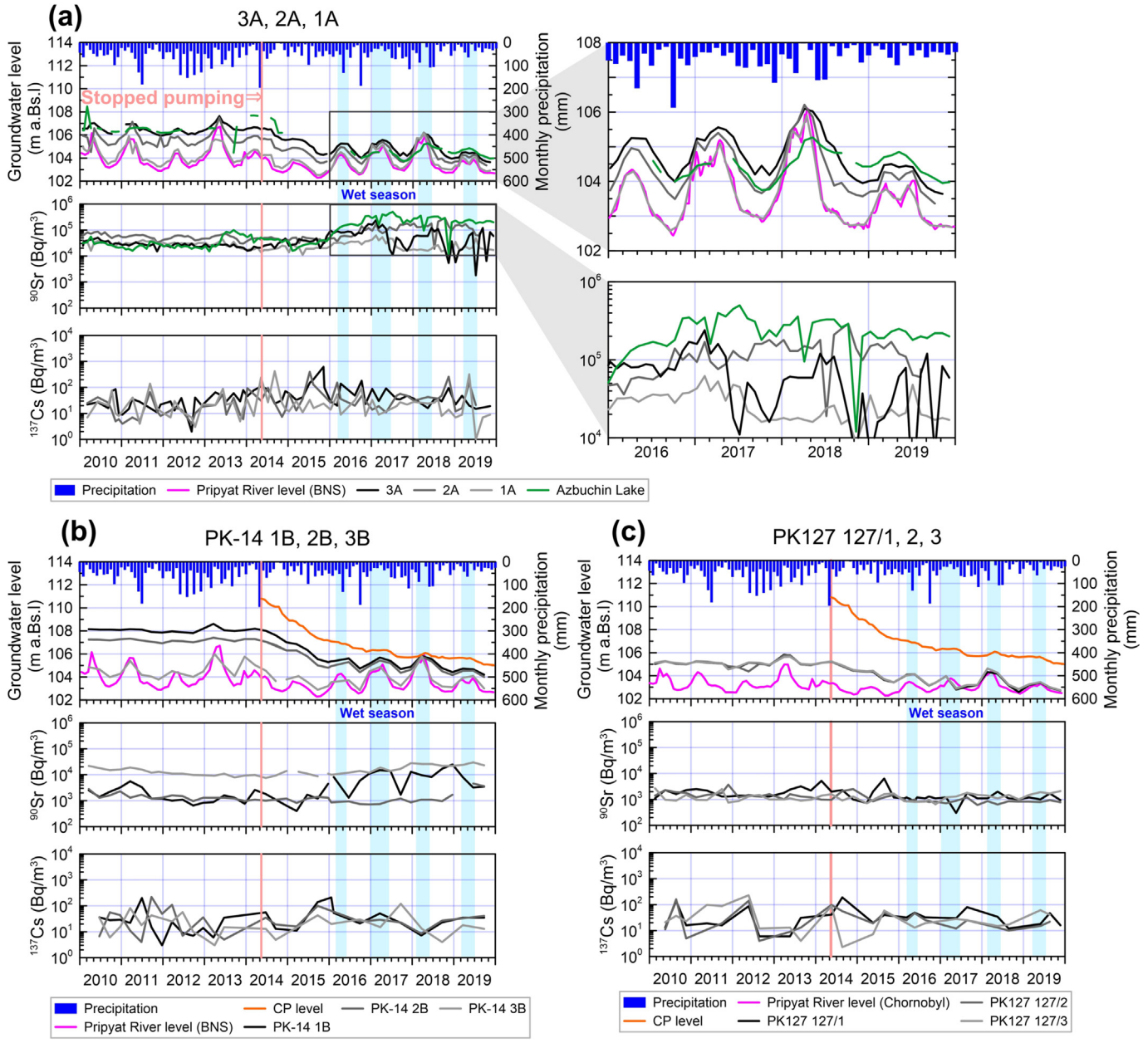

Fig. 4. Time series of precipitation, groundwater levels (m a.Bs.l), and ^{90}Sr and ^{137}Cs concentrations in selected wells north and east of the CP before and after the drawdown, which is shown by the vertical pink line. The blue bands indicate the "wet season" due to snow melt, when river levels were high due to snow melt. The locations of these wells are indicated in Fig. 3c. (For interpretation of the references to colour in this figure legend, the reader is referred to the web version of this article.)

and 2A increased by approximately 10 times (Fig. 4a). This corresponds to the timing and magnitude of the increase in ^{90}Sr concentrations in Azbuchin Lake. As shown in Fig. 4b, at PK-14 wells, the ^{90}Sr concentrations were approximately 10^4 Bq/m^3 at well 3B and 10^3 Bq/m^3 at wells 1B and 2B from 2010 to 2013. However, all three PK-14 wells showed an increase in ^{90}Sr concentrations after the CP drawdown, especially 1B, which is the closest to the CP. As shown in Fig. 4c, ^{90}Sr concentrations in the nested well PK-127 were approximately 10^3 Bq/m^3 without significant changes owing to the CP drawdown.

From the middle panels in Fig. 5, we identified decreasing or consistent seasonal trends in ^{90}Sr concentrations after the CP drawdown. As shown in Fig. 5a, ^{90}Sr concentrations at well 2/1 increased before 2012, with a temporary further increase from 10^5 to 10^6 Bq/m^3 at the end of 2013 and 2014 due to heavy precipitation in 2012–2013. However, ^{90}Sr concentrations decreased to 10^4 Bq/m^3 after the CP drawdown (Fig. 5a). As shown in Fig. 5b and c, ^{90}Sr concentrations in wells 168 and 193 showed no significant changes before or after the CP drawdown.

The ^{137}Cs concentrations were between 10^1 and 10^2 Bq/m^3 at all selected wells (Figs. 4 and 5), which is 1–3 orders of magnitude lower than the ^{90}Sr concentrations. In addition, ^{137}Cs concentrations did not significantly change after the decommission of the CP.

4.3. Changes in groundwater levels and direction

Changes in the groundwater regime due to the CP drawdown were evaluated at the monitoring wells and are illustrated by groundwater-level contours during the dry season (Fig. 6). In Fig. 6a, the groundwater-level contours are shown for January 2014, when the CP was in operation, and Fig. 6b shows the groundwater-level contours for January 2019, which was after the CP drawdown. The 3-year average precipitation at the

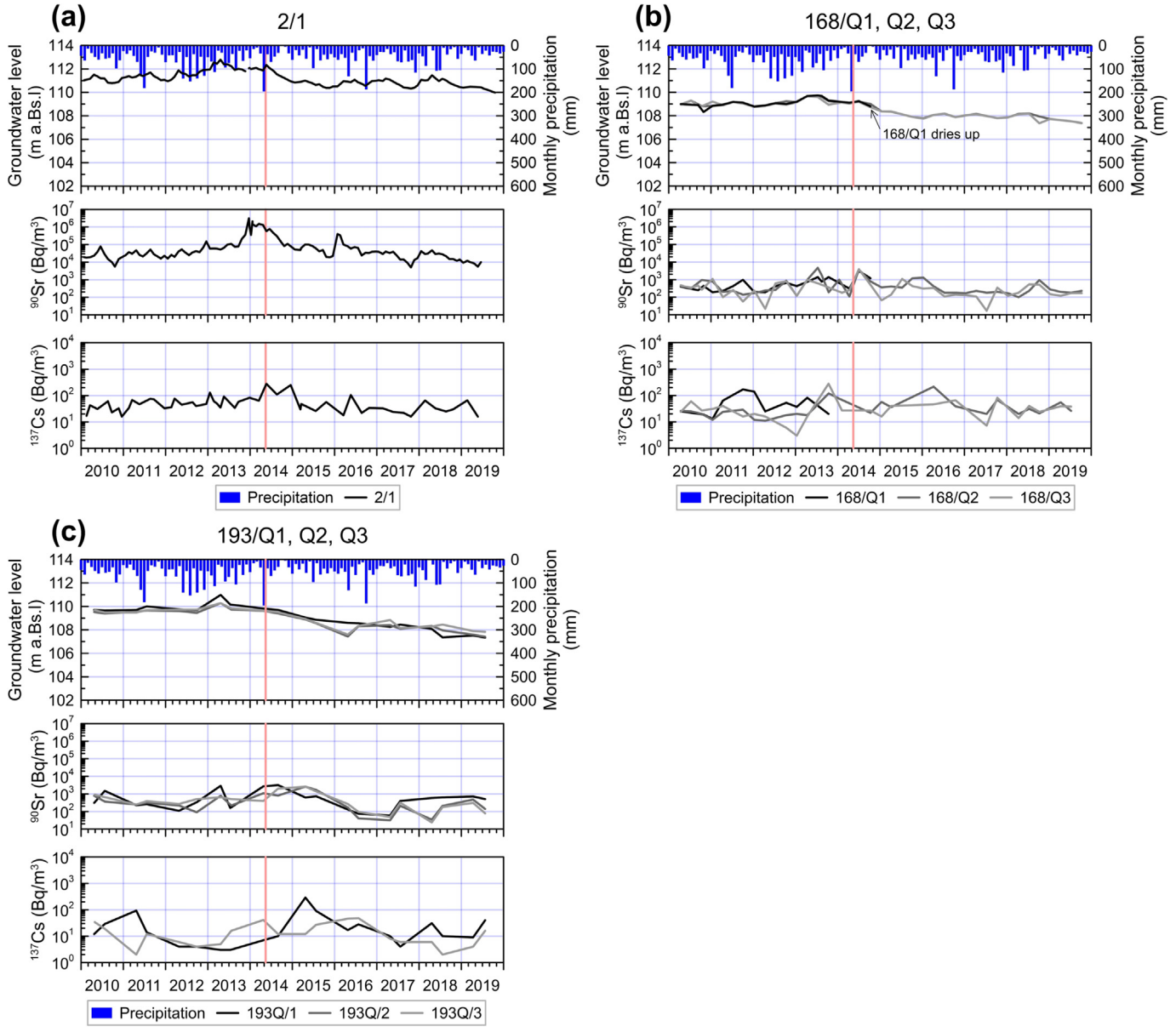

Fig. 5. Time series of precipitation, groundwater levels (m a.Bs.l), and ^{90}Sr and ^{137}Cs concentrations in the selected wells west and south of the CP before and after the drawdown, which is shown by the vertical pink line. The locations of these wells are indicated in Fig. 3c. (For interpretation of the references to colour in this figure legend, the reader is referred to the web version of this article.)

ChNPP was 1.6 times higher during 2011–2013 (773 ± 44 mm) than that during 2017–2019 (496 ± 29 mm); the 2014–2016 period had a 3-year average precipitation of 603 ± 43 mm. The winter season is dry, with monthly average air temperatures significantly below 0 °C (January 2014: −5.7 °C, January 2019: −4.7 °C). January was selected because it was minimally affected by rainfall. The average precipitation values for the three months immediately prior to January 2014 and 2019 were 36.6 ± 20.8 mm and 26.7 ± 21.9 mm, respectively, and the monthly average water levels of the Pripyat River measured at the BNS site were 103.95 ± 0.07 m and 103.10 ± 0.14 m a.Bs.l, respectively.

Prior to the CP drawdown, the groundwater gradient was influenced by infiltration from the CP. Local groundwater flowed north from the CP to Azbuchin Lake (Fig. 6a). In January–April 2014, when the CP was still operating, the surface water level in the CP was approximately 111 m a.Bs.l; thus, the difference between the CP and Pripyat River was approximately 7 m. In Fig. 6a, a steep groundwater gradient can be seen on the east and north sides of the CP, which had the fastest groundwater velocity in this area. In addition, the CP water levels influenced the regional groundwater flow on the western side of the CP, creating a groundwater stagnation area south of the ChNPP (Fig. 6a). Therefore, contaminated surface water in the CP was a major source of groundwater recharge and influenced the local and regional groundwater gradients.

The water level in the CP decreased to 105.6 m a.Bs.l. in January 2019. The area north of the CP no longer flows from the CP and has been replaced by direct flow from the ChNPP to the Pripyat River. In addition, the distance between the water-level contours increased and the flow velocity decreased. On the east and north sides of the CP, the contours demonstrate much smaller gradients, as shown by the wide separation in Fig. 6b. In contrast, on the west side of the CP, the contours resulted from the regional gradient, and the decline in water levels in the CP resulted in faster velocities than before the CP was decommissioned.

Estimated changes in groundwater levels between January 2014 and January 2019 are shown in Fig. 6c. A 50 cm change in groundwater levels was identified at approximately 65 % of the monitoring wells. Changes of 5 m occurred near the CP, as indicated by the extended concentric circles (Fig. 6c). Contour lines indicating 1 m of change in groundwater levels

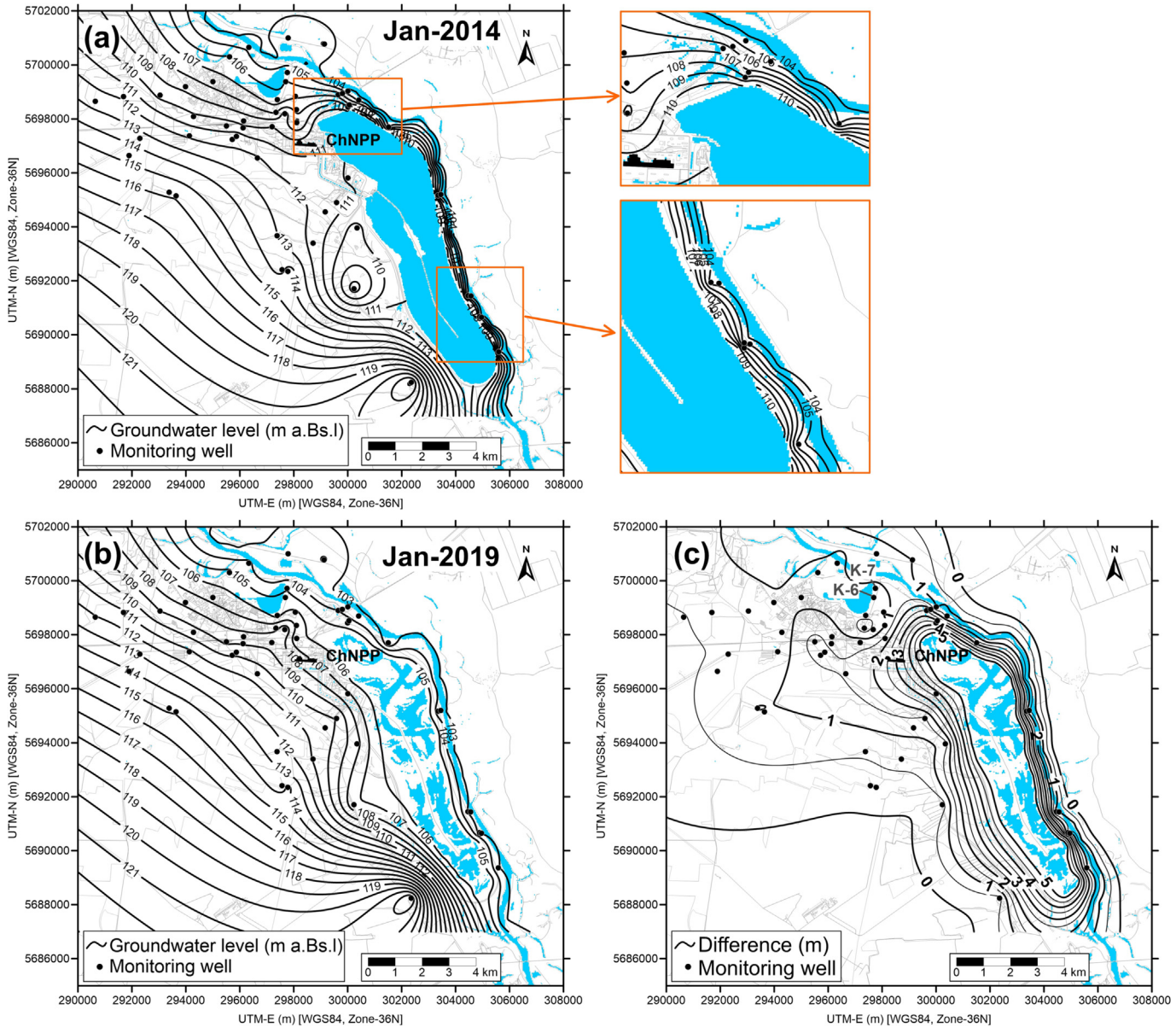

Fig. 6. Groundwater level contours (m a.Bs.l.) of the unconfined aquifer monitoring wells on (a) January 2014 and (b) January 2019 and (c) the difference between them (m). Enlarged views of the north and southeast of the CP were shown on the right side of panel (a). The water areas were mapped by selected low cloud-cover Landsat8 C2L2 (QA_PIXEL) images (a: as of March 9, 2014; b and c: as of May 19, 2019) downloaded from the USGS EarthExplorer (https://earthexplorer.usgs.gov/).

extended westward from the CP to the western area of the ChNPP. Only small changes of several tens of centimeters before and after the CP drawdown were observed surrounding the Pripyat backwater, which is located 2-km away from the northern tip of the CP.

5. Discussion

5.1. Evaluating changes before and after CP drawdown

The CP drawdown stopped artificial recharge to the unconfined aquifer, resulting in the reduction of groundwater levels and velocities, changes in groundwater flow direction, and altered groundwater-surface water interactions. During the CP operation, high water levels of 111 m a.Bs.l. were maintained in the CP by the continuous pumping via four pumps at approximately 3.17 m^3/s each from the Pripyat River (IAEA, 2019). Hence, water seeped from the CP via the north and south drainage canals and leaked into the shallow unconfined aquifer. Since November 2014, the CP water level has been gradually declining, reducing the seepage; moreover, the northern and southern drains stopped flowing in 2017 due to the decline in water level below their elevation. The current surface water area of the CP has been reduced to three lacustrine wetlands formed above the low-permeability CP bottom, and groundwater leakage via the CP bottom sediments is the only pathway for radionuclide migration. The changes in the CP leakage had most influence during the dry season, extending as far as 3 km away. The magnitude of this change was up to 6 m at the edge of the former CP (Fig. 6c). Based on the characteristic leakage length λ (Gusyev and Haitjema, 2011) and the CP leakage extent demonstrated in Fig. 6c, the northern area of the CP had two times higher leakage length to the northern and eastern sides than that of the southern area of the CP. Moreover, this leakage factor difference indicates four times higher hydraulic conductivity of the CP bottom sediments between northern and southern CP areas. This is an important consideration, as the northern area of the CP had the most nuclear fuel particles deposited in 1986, and the Pripyat floodplain, with several small lakes, had RWTSP containing buried highly radioactive waste (Ledenev et al., 1995; IAEA, 2019).

In the current regime, surface water level of the lacustrine wetlands within the CP fluctuates due to wet- and dry- season precipitation levels, becoming a driving process in surface water–groundwater interactions. During the wet season, rainfall accumulates in small ponds, resulting in an increase in surface water levels, which increases seasonal leakage to the shallow unconfined aquifer, thereby increasing groundwater velocity compared to the regional groundwater flow. In addition, wet season precipitation may create groundwater mounding that locally affects groundwater flow direction, such as groundwater mounding at the Pripyat River floodplain with two opposite groundwater flow directions to the Pripyat River and Azbuchin Lake. For example, groundwater levels can fluctuate up to 2 m between the wet and dry seasons as observed in well 3A (Fig. 4a) and could potentially cause the vertical and horizontal inflow of ^{90}Sr and ^{90}Sr mobilization from sediments to water due to the change in water hydrochemistry. The high water levels of the Pripyat River, which has higher concentrations of dissolved ^{90}Sr and ^{137}Cs during the high flow season (Bugai et al., 2022), are above groundwater levels, such as well 3A in Fig. 4a, indicating a reversal of the hydraulic gradient from the Pripyat River to nearby wells during the wet season. As a result of these seasonal changes in the groundwater flow direction and gradients, the dissolved inflow of ^{90}Sr may move much slower than groundwater of the unconfined aquifer, explaining the increasing ^{90}Sr concentrations in these wells (Fig. 4). This activated recharge continues for several weeks, with declining surface area and water levels in the ponds due to seepage and evapotranspiration.

For the dry months, the influence of the CP infiltration on the local groundwater system has nearly stopped before and after the CP drawdown due to the reduced leakage from the CP bottom. Prior to the drawdown, the groundwater flow direction in the shallow aquifer was from the CP to Azbuchin Lake and Pripyat River and the CP leakage was creating a hydraulic barrier of groundwater with low radionuclide concentrations. This hydraulic barrier was preventing groundwater and radionuclide movement from the area north of ChNPP to Azbuchin Lake and Pripyat River. After the CP drawdown, the artificial leakage of CP surface water stopped making the regional groundwater flow a dominant process of radionuclide transport from southwest to northeast. In the northern area of the CP reservoir, the natural water levels of the lacustrine wetlands are only up to 2 m higher than Pripyat water levels at BNS river gauge suggesting that a direct hydraulic connection still exists between the CP and Pripyat River with much slower groundwater velocities. These seasonal fluctuations of CP, Azbuchin Lake, and Pripyat River water levels could be the driving processes responsible for the increase of ^{90}Sr radionuclide concentrations in monitoring wells at the Pripyat floodplain. This process is also supported that ^{90}Sr concentrations of Azbuchin Lake have a much larger increase compared to the CP water after the CP drawdown as discussed in the next section. Since groundwater flow is the main transport of ^{90}Sr radionuclides to the Pripyat River in dry months, the continuous monitoring of the radionuclide hazard based on actual groundwater levels is needed for understanding the groundwater influence on the Pripyat River concentrations in the future.

5.2. Radionuclide concentration changes in the CP, lake, and groundwater

The decrease in water level in the CP significantly affected the surrounding groundwater level and flow (Fig. 6). High ^{90}Sr concentrations in the groundwater west of the ChNPP before the CP drawdown decreased afterwards. A 1-m decrease in the groundwater table resulted in lower concentrations presumably due to groundwater decreases to below the shallow highly contaminated layer (Bugai et al., 2022). In the area between the CP and Pripyat River, the changes in ^{90}Sr were very small, approximately −100 %, except for PK-14 1B, which caused the decrease in the hydraulic gradient and the small increase in ^{90}Sr in CP water (Fig. 7). Therefore, we focused on the factors contributing to the more pronounced increase in concentration north of the CP.

North of the CP (wells north of 3A and Azbuchin Lake), the ^{90}Sr concentrations were the highest near the Pripyat River, ranging from 5.0×10^4 to 3.5×10^5 Bq/m^3 which is above the WHO drinking water guideline of 10 kBq/m^3 (WHO, 2017) (Fig. 7a and c). In Fig. 1, this area had a high initial deposition (Kashparov et al., 2018), and the difference of ^{90}Sr concentrations could be related to the amount of the initial deposition (Fig. 7b and c). In particular, the ^{90}Sr concentrations in Azbuchin Lake and wells 3A and 2A were affected by reduced flow from the CP with lower ^{90}Sr concentrations and chemical reactions of fuel particles due to the lowering of water levels in the surrounding ponds (Bulgakov et al., 2009). In addition, it is possible that contaminants generated from unidentified waste trenches in the past may also contribute as the source. The additional increase in ^{90}Sr is also noteworthy because the flow direction is now the original flow direction along the topography from the ChNPP, RWDS and RWTSP to the Pripyat River and Azbuchin Lake. However, the present results show no increase in ^{90}Sr in the vicinity of the "Podlesny" RWDS. This is thought to be due to the groundwater table decline from the highly contaminated layer due to the CP drawdown.

Water levels at Azbuchin Lake and Pripyat backwater changed by approximately 2 m and 0.5 m between the two periods, respectively. Water volume changes could be a factor in the increased ^{90}Sr concentrations in Azbuchin Lake; hence, the concentration of ^{137}Cs should also have increased by the same ratio. However, the changes in the ^{137}Cs concentrations in Azbuchin Lake and Pripyat backwater were smaller (65 % and 6 %, respectively) than those of the ^{90}Sr concentrations (653 % and −28 %, respectively) as shown in Supplementary Table S2 and S4. Therefore, the ^{90}Sr concentrations are likely increased because of transport rather than volume changes.

The shallower well 2A and deeper well 2 located near Azbuchin Lake show increasing of ^{90}Sr concentrations that is likely due to the transport from the Azbuchin Lake bottom due to approximately the same groundwater levels in both wells. In previous study, Bugai et al. (2022) found "no trend" in the ^{90}Sr concentrations in wells 2A and 2 using long-term annual data, whereas our results suggest the importance of interannual variability before and after the CP drawdown. The concentrations at K-7 and K-6 near the Pripyat River were also elevated by 300 % and 600 %, respectively, despite a small decrease in groundwater level (Figs. 3d and 6c). Nevertheless, this finding is consistent with the increasing long-term trend observed by Bugai et al. (2022). The wells with increasing ^{90}Sr concentrations unrelated to groundwater decline are located near Pripyat backwater, which is highly contaminated by radioactive fallout on its water surface and surrounded by nuclear waste trenches at the "Neftevaza" RWTSP, as mentioned in Section 2.3. The high radionuclide concentrations in this area could have been caused by the dissolution of fuel particles in the trenches and Pripyat backwater (Bulgakov et al., 2009) and their subsequent transport to groundwater (Bugai et al., 2022). This mechanism is supported by the lack of increases in ^{137}Cs concentrations, and presence of ^{90}Sr, due to differences in mobilities (Kd value) (Bugai et al., 2020). Additionally, this result indicates that the increase in ^{90}Sr concentrations in groundwater near Azbuchin Lake cannot be explained solely by leaching from the trenches, because trenches are absent in the vicinity of Azbuchin Lake.

Increase of ^{137}Cs radionuclide has a completely different mechanism than ^{90}Sr mobilization due to the difference in Kd values (Bugai et al., 2020). Indeed, the location of the wells with increased ^{137}Cs change ratios (Supplementary Fig. S1d) was different from those with increased ^{90}Sr. In addition, ^{137}Cs concentrations did not change at the sites where ^{90}Sr was significantly increased (Figs. 4 and 5). It is very interesting that the only three sites with high change ratios above 300 % were in the vicinity of radioactive waste facilities, despite the large and rapid groundwater drawdown due to CP decommissioning. In Fig. 7b, ^{137}Cs concentrations in CP water have increased 1.5 to 2 times since 2015 after the drawdown and the concentrations are higher than in the groundwater, about 1×10^3 Bq/m^3 in 2015–2019. The ^{137}Cs increase in the CP water was explained by different mechanisms, such as reduced self-purification, increased biomass density, and oxidized fuel particles due to lowered water levels (Bulgakov et al., 2009; IAEA, 2019). In this study, the sites where significant rates of change occurred are identified around RWDS. In addition, increased ^{137}Cs concentrations are also observed in groundwater at depths of

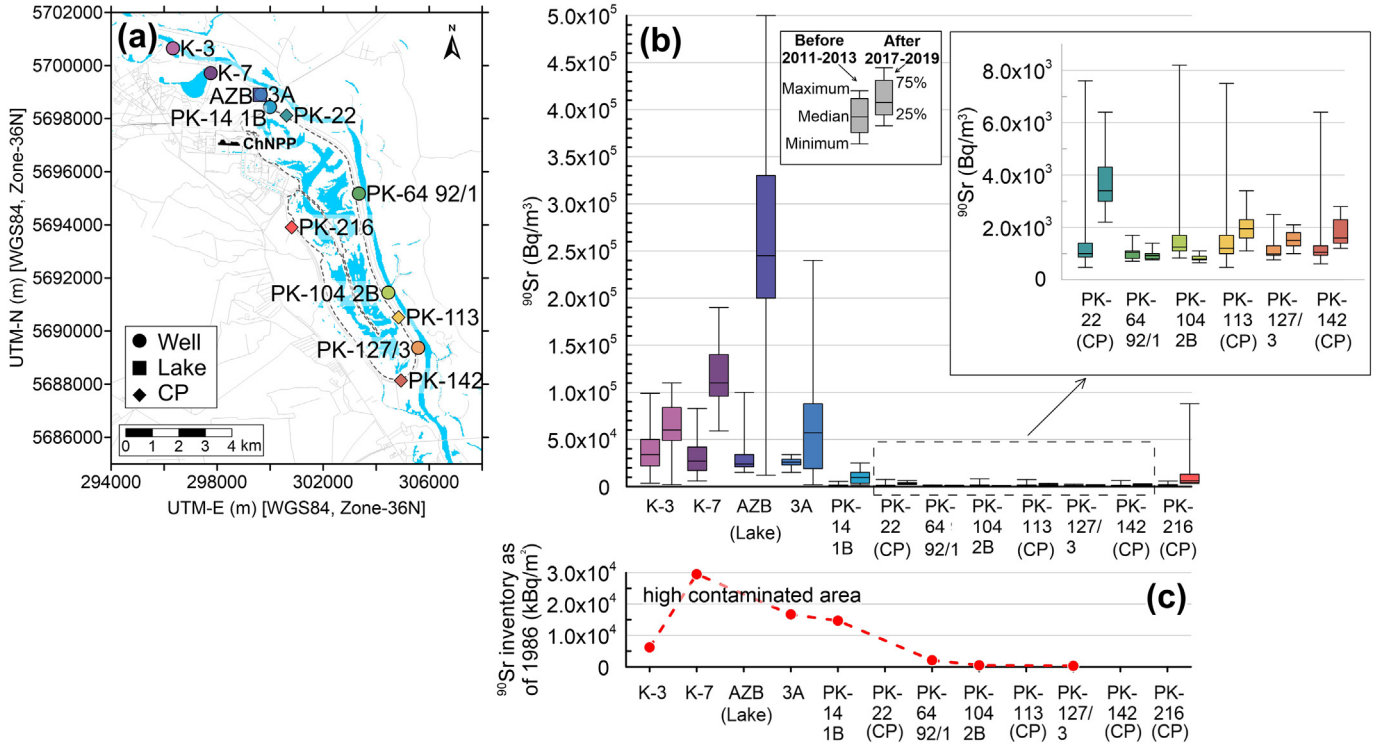

Fig. 7. Changes in ^{90}Sr concentrations in groundwater and surface water of the CP and lakes. (a) ^{90}Sr concentrations were analyzed in the groundwater, lakes, and CP at a total of 12 sites. (b) Changes in the average ^{90}Sr concentration for three years before (2011–2013) and after (2017–2019) the CP decommission, which were related to ^{90}Sr deposition (kBq/m^2) near the CP (c). The deposition was estimated by inverse estimation using half-life based on the database of Kashparov et al. (2018). In panel (b), the box-and-whisker plots were colored by the same colour coding at the same points, with the concentrations on the left before the drawdown and on the right after the drawdown. The water areas in the panel (a) is mapped using selected low cloud-cover Landsat8 C2L2 (QA_PIXEL) images (as of May 19, 2019) downloaded from the USGS Earth Explorer (https://earthexplorer.usgs.gov/). Sample name of AZB indicates Azbuchin Lake. (For interpretation of the references to colour in this figure legend, the reader is referred to the web version of this article.)

about 30 m. This may be caused by artificial factors (e.g., cross-contamination from surface, flow along the well, etc.) and several natural factors including colloids transport or complexes in relatively deep groundwater, as noted by Bugai et al. (2022). The mechanisms causing presence of relatively immobile Cs in monitoring wells are not fully understood and this study only suggests that increased ^{137}Cs concentrations are associated with the location of radioactive waste.

5.3. ^{90}Sr transport to the Pripyat River before and after the CP drawdown

Data regarding the ^{90}Sr concentrations transported from the CP to the Pripyat River are needed for downstream impact assessments; therefore, we analyzed the ^{90}Sr fluxes for 1999–2019 using data collected from the monitoring wells at the floodplain between the CP and the Pripyat River and near Azbuchin Lake. Using the approach of Bugai and Skalskky (2013) as described in Section 3.3, the calculated area is as shown in Supplementary Fig. S2, and the changes in the groundwater flow regime with decreased discharge and increased traveling times are listed in Supplementary Table S7.

Considering groundwater discharge without the delay due to the retardation factor, the ^{90}Sr fluxes from wells installed near the CP and Azbuchin Lake from 1999 to 2019 changed from 0.078 ± 0.024 to 0.020 ± 0.012 TBq/m^3 and from 0.053 ± 0.061 to 0.014 ± 0.003 TBq/m^3, respectively. After the CP drawdown, they decreased by approximately 70 % compared to those at the beginning of the measurement (Supplementary Table S6). The estimated ^{90}Sr flux in the CP area from 1999 to 2010 was 10^{10}–10^{11} Bq/m^3, which is similar to the values published by Bugai and Skalskky (2013) calculated before drawdown, although the velocity calculation differed. Well PK-14 3B, which is north of the CP, has experienced increasing ^{90}Sr concentrations since 2016; the 3-year average after the CP drawdown was double that before, as shown in Fig. 3 and Fig. 4B. However, a comparison of fluxes over this period showed a 3 % decrease. This is evidence that the reduction in the hydrodynamic gradient contributed significantly to the reduction in ^{90}Sr flux. In contrast, in well 1A near Azbuchin Lake, the concentrations decreased by approximately 20 % and fluxes decreased by 30 % from before to after the CP drawdown.

When the delay due to the retardation factor was considered, the ^{90}Sr flux calculated at wells near the CP and Azbuchin Lake decreased slowly (Fig. 8a). Transport time from wells near the CP to the Pripyat River changed from 5 to 8 y in the north (PK-14) and from 0.5–9 y to 1.5–217 y in the south (PK-32, 64, and 113) (Supplementary Table S7). In Fig. 8b, the contribution of the CP area based on four wells has approximately 10 % in 2015 and 2–6 % from 2014 to 2019 of the ^{90}Sr flux in the Pripyar River (Supplementary Table S8). This reflects the past ^{90}Sr flux, which was due in part to the effect of the delay; therefore, there are were significant changes between the periods before and after the CP drawdown. In PK-14, where the concentration increased by approximately 3 % after the CP drawdown, the transport time changed from 5 to 8 y. Considering the half-life of ^{90}Sr (28.8 years), the concentration would decrease by 17 % over 8 y; therefore, the delay further decreased the concentration. Thus, the wells near the CP show reduced discharge and retardation effects owing to the lowered hydraulic gradient; moreover, the ^{90}Sr flux is expected to decrease in the future. If the additional ^{90}Sr from the CP flowed into Pripyat, the effect of ^{90}Sr transport from the CP would be small because the flux from CP to the river, as estimated by Bugai and Skalskky (2018), should not exceed 0.7 GBq/y. Transport time at 1A, near Azbuchin Lake, increased from 0.4 to 0.6 y after the CP discharge and immediately discharged to the river; contributions from 1A to the river were 1–3 % after the CP water level drop, with an increase of about 30 % compared to 3 years before and after the CP drawdown. This may be because the flux at 1A did not change significantly, whereas the flux in the river itself decreased (IAEA, 2019; Igarashi et al., 2020, Supplementary Table S8).

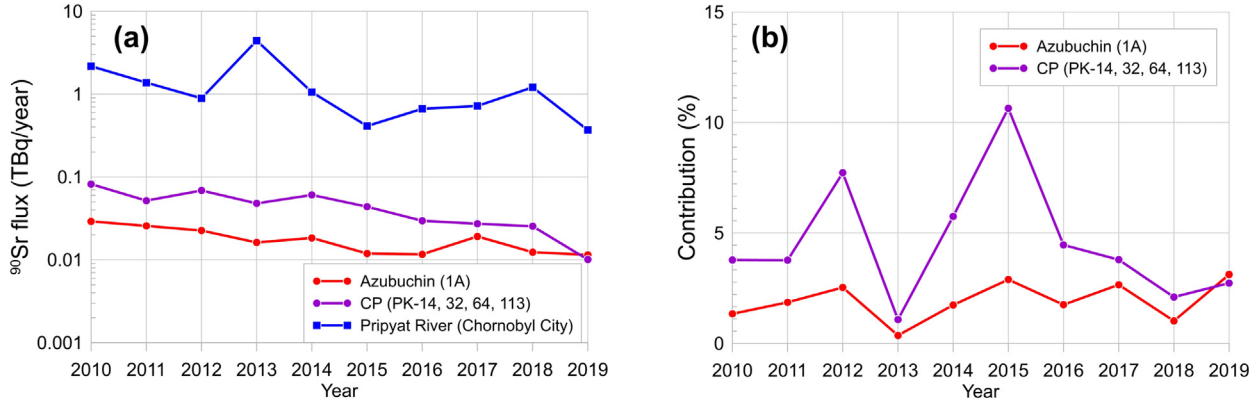

Fig. 8. The ^{90}Sr annual flux (a) and contribution (b) at Chornobyl City monitoring site of the Pripyat River from Azbuchin Lake and cooling pond (CP) areas from 2010 to 2019.

The contributions of estimate area at ChEZ up to 2019 were below 10 % with little change. This is because ^{90}Sr flux in the Pripyat River and the tributary river also decreased with ^{90}Sr flux in groundwater (IAEA, 2019; Igarashi et al., 2020). The remaining approximately 90 % is considered to be contributed by ^{90}Sr transport from surface water and groundwater other than the estimated areas shown in Supplementary Fig. S2. The State Specialized Enterprise Ecocentre measured ^{90}Sr concentrations in the Pripyat River at the ChEZ inlet and outlet, located at the Ukraine–Belarus border and the city of Chornobyl, respectively (Kireev et al., 2013; Bugai et al., 2022). According to this data, the ^{90}Sr fluxes received by the Pripyat River inside the ChEZ have decreased since 2015, while the groundwater contributions from the CP and Azbuchin areas to the river did not change, rising only about 2 % each after the drawdown (Supplementary Table S9). Bugai et al. (2022) indicates that 80–90 % of the ^{137}Cs flux transports from upstream of the ChEZ and 50–70 % of the ^{90}Sr flux transports within the ChEZ, and describes the ^{90}Sr concentration is controlled by the discharge from surface waters. Our results also support the finding of reduced radionuclide transport to the Pripyat River after the CP drawdown predicted by Buckley et al. (2002). Based on these results, we consider that the impact from groundwater to the river is small even after the drawdown. However, the ^{90}Sr flux in groundwater may increase slightly in the future because of additional transport as mentioned in Section 5.2. Therefore, monitoring should focus on the highly concentrated areas near the small lakes in the northern area of the CP and the ^{90}Sr flux should be validated by groundwater flow models for accurate flux estimations.

6. Conclusions

This is the first study to quantitatively evaluate the spatial distributions and time-series trends in groundwater levels and ^{137}Cs and ^{90}Sr radionuclide concentrations in the shallow unconfined aquifer before and after the CP drawdown. The analyses were performed on observational data from 2010 to 2019 in the vicinity of the ChNPP, and we observed that the natural drawdown of the CP had been affecting the surrounding groundwater system since May 2014. This study confirmed that ^{137}Cs concentrations did not significantly change before and after the drawdown. The new finding of this study is that the average ^{90}Sr concentrations increased north of the ChNPP in the Pripyat River floodplain including Azbuchin Lake and decreased east and west of the CP between 2011–2013 and 2017–2019 time periods. This finding was counterintuitive since the CP drawdown resulted in a decline in groundwater levels, changes in groundwater velocity, and a shift in the groundwater flow direction, as the CP water levels dropped by 6 m. In addition, the current trends of increasing ^{90}Sr concentrations that were established from the available data are useful for future field investigations of groundwater and lakes in the vicinity of the CP.

Although CP drawdown was considered expedient for preventing groundwater flow contamination by radionuclides, our results support the hypothesis that the increase in ^{90}Sr concentrations in the Pripyat River floodplain can be attributed to the decrease in dilution rate from the CP due to the decreased leakage and the change in groundwater flow direction as well as the decrease in groundwater velocity. Our study also revealed changes in ^{90}Sr transport from 2010 to 2019 by groundwater near the CP and Azbuchin Lake, which were feared to become highly contaminated sources of the radioactivity, to the Pripyat River. From the new finding of this study that the drawdown increased ^{90}Sr concentrations near the floodplain, we estimated the ^{90}Sr flux and contribution to the Pripyat River and the ^{90}Sr contribution did not change significantly after the drawdown. Although increased concentrations were observed in the floodplain, they are not expected to have a significant impact on the Pripyat River due to the delay in transport caused by the lowering of the hydrodynamic gradient. However, north of the ChNPP in the Pripyat River floodplain, ^{90}Sr concentrations in groundwater may increase gradually due to the vertical and horizontal inflow of ^{90}Sr as well as the ^{90}Sr mobilization in the future. The total ^{90}Sr flux in the area between the CP and the Pripyat River and near Azbuchin Lake could still contribute up to 10 % of the ^{90}Sr flux in the Pripyat River. Therefore, it is necessary to continuously monitor ^{90}Sr concentrations and groundwater levels in the wells and lakes, and establish monitoring wells within the CP area to measure leakage rates from the lacustrine wetlands.

CRediT authorship contribution statement

Hikaru Sato: Conceptualization, Methodology, Validation, Investigation, Writing - Original Draft Visualization. **Maksym Gusyev:** Conceptualization, Methodology, Validation, Writing - Original Draft, Review & Editing. **Dmytro Veremenko:** Investigation, Data Curation. **Gennady Laptev:** Investigation, Data Curation, Writing - Review & Editing. **Naoaki Shibasaki:** Writing - Review & Editing, Supervision. **Yuichi Onda:** Writing - Review & Editing. **Mark Zheleznyak:** Supervision. **Serhii Kirieiev**: Resources, Supervision. **Kenji Nanba:** Supervision, Funding acquisition.

Data availability

Data will be made available on request.

Declaration of competing interest

The authors declare that they have no known competing financial interests or personal relationships that could have appeared to influence the work reported in this paper.

Acknowledgments

This work was supported by the Japanese government (JST/JICA) program for international joint research into global issues, called the Science

and Technology Research Partnership for Sustainable Development JST-JICA, Japan (SATREPS project, PI. Kenji Nanba; grant number JPMJSA1603). We thank Dr. Haruko Murakami for the useful discussions about the migration of radionuclides and Dr. Dmitri Bugai for providing materails on Chernbyl site and cooling pond hydrogeology. We are grateful to five anonymous Reviewers for their constructive comments that have greatly improved the manuscript. We also thank all staff of SSE Ecocentre in Chornobyl for their continuous monitoring and analysis of radionuclide concentrations.

Appendix A. Supplementary data

Supplementary data to this article can be found online at https://doi.org/10.1016/j.scitotenv.2023.161997.

References

Beresford, N.A., Fesenko, S., Konoplev, A., Skuterud, L., Smith, J.T., Voigt, G., 2016. Thirty years after the Chernobyl accident: what lessons have we learnt? J. Environ. Radioact. 157, 77–89. https://doi.org/10.1016/j.jenvrad.2016.02.003.

Bixio, A.C., Gambolati, G., Paniconi, C., Putti, M., Shestopalov, V.M., Bublias, V.N., Bohuslavsky, A.S., Kasteltseva, N.B., Rudenko, Y.F., 2002. Modeling groundwater-surface water interactions including effects of morphogenetic depressions in the Chernobyl exclusion zone. Environ. Geol. 42, 162–177. https://doi.org/10.1007/s00254-001-0486-7.

Buckley, M.J., Bugai, D., Dutton, L.M.C.D., Gerchikov, M.Y., Kashparov, V.A., Ledenev, A., Voitzehovich, O., Weiss, D., Zheleznyak, M., 2002. Drawing up and evaluating remediation strategies for the Chernobyl cooling pond. Final Report, Issue 01, Rep. no. C6476/TR/01. NNC Limited, Manchester https://doi.org/10.13140/RG.2.1.1263.3840.

Bugai, D., Dewiere, L., Kashparov, V.A., Ahamdach, N., 2002. Strontium-90 transport parameters from source term to aquifer in the Chernobyl Pilot Site. Radioprotection 37. https://doi.org/10.1051/radiopro/2002024 C1-11-16.

Bugai, D., Kireev, S., Hoque, M.A., Kubko, Y., Smith, J., 2022. Natural attenuation processes control groundwater contamination in the Chernobyl exclusion zone: evidence from 35 years of radiological monitoring. Sci. Rep. 12, 18215. https://doi.org/10.1038/s41598-022-22842-5.

Bugai, D.A., Skalskiy, A.S., Dzhepo, S.P., 2007. Water protection measures for radioactive groundwater contamination in the CEZ. In: Onishi, Y., Voitsekhovich, O.V., Zheleznyak, M.J. (Eds.), Chernobyl - What Have We Learned?. Environ. Pollut., 12. Springer, Dordrecht https://doi.org/10.1007/1-4020-5349-5_7.

Bugai, D.A., Skalskky, A.S., 2013. Numerical modeling of hydrogeological conditions resulting from the Chernobyl NPP cooling pond decommissioning and remediation. Report on the IAEA Contract no.201301006-EG. Geo-Eco-Consulting Ltd, Kyiv in Russian.

Bugai, D.A., Skalskky, A.S., 2018. Radionuclide transport in groundwater from the cooling pond of Chernobyl NPP to Pripyat River: retrospective analysis and modeling prediction following pond decommissioning. 2018 Problems of Chernobyl Exclusion Zone, Issue no. 18, 2018. Chernobyl Center for Problems of Nuclear Safety Radioactive Waste and Radioecology, Slavutich, pp. 60–66 in Russian.

Bugai, D., Skalskyy, A., Dgepo, S., Oskolkov, B., 2005. Experimental hydrogeological studies and filtration analyses for the Chernobyl cooling pond. Bulletin of the ecological status of the Chernobyl exclusion zone. 1, pp. 45–56 (in Ukrainean).

Bugai, D., Skalskyy, A., Dzhepo, S., Kubko, Yu., Kashparov, V., Van, M.N., Stammose, D., Simonucci, C., Martin-Garin, A., 2012a. Radionuclide migration at experimental polygon at red Forest waste site in Chernobyl zone. Part 2: hydrogeological characterization and groundwater transport modeling. Appl. Geochem. 27, 1359–1374. https://doi.org/10.1016/j.apgeochem.2011.09.028.

Bugai, D., Smith, J., Hoque, M.A., 2020. Solid-liquid distribution coefficients (Kd-s) of geological deposits at the Chernobyl nuclear power plant site with respect to Sr, Cs and Pu radionuclides: a short review. Chemosphere 242, 125175. https://doi.org/10.1016/j.chemosphere.2019.125175.

Bugai, D., Tkachenko, E., Van, M.N., Simonucci, C., Martin-Garin, A., Roux, C., Le Gal La Salle, C., Yu, Kubko, 2012b. Geochemical influence of waste trench no.22T at Chernobyl pilot site at the aquifer: long-term trends, governing processes, and implications for radionuclide migration. Appl. Geochemistry. 27, 1320–1338. https://doi.org/10.1016/j.apgeochem.2011.09.021.

Bugai, D.A., Waters, R.D., Dzhepo, S.P., Skalsk'ij, A.S., 1997. The cooling pond of the Chernobyl nuclear power plant: a groundwater remediation case history. Water Resour. Res. 33, 677–688. https://doi.org/10.1029/96WR03963.

Bulgakov, A., Konoplev, A., Smith, J., Laptev, G., Voitsekhovich, O., 2009. Fuel particles in the Chernobyl cooling pond: current state and prediction for remediation options. J. Environ. Radioact. 100, 329–332. https://doi.org/10.1016/j.jenvrad.2008.12.012.

Dai, M., Kelley, J.M., Buesseler, K.O., 2002. Sources and migration of plutonium in groundwater at the Savannah River site. Environ. Sci. Technol. 36, 3690–3699. https://doi.org/10.1021/es020025t.

Dewiere, L., Bugai, D., Grenier, C., Kashparov, V., Ahamdach, N., 2004. ^{90}Sr migration to the geo-sphere from a waste burial in the Chernobyl exclusion zone. J. Environ. Radioact. 74, 139–150. https://doi.org/10.1016/j.jenvrad.2004.01.019.

Fredrickson, J.K., Zachara, J.M., Balkwill, D.L., Kennedy, D., Li, S.W., Kostandarithes, H.M., Daly, M.J., Romine, M.F., Brockman, F.J., 2004. Geomicrobiology of high-level nuclear waste-contaminated vadose sediments at the Hanford site, Washington state. Appl. Environ. Microbiol. 70, 4230–4241. https://doi.org/10.1128/AEM.70.7.4230-4241.2004.

Gusyev, M.A., Haitjema, H.M., 2011. An exact solution for a constant-strength line-sink satisfying the modified Helmholtz equation for groundwater flow. Adv. Water Resour. 34, 519–525. https://doi.org/10.1016/j.advwatres.2011.01.009.

International Atomic Energy Agency (IAEA), 2006. Environmental Consequences of the Chernobyl Accident and their Remediation: Twenty Years of Experience. Radiological Assessment Reports Series No. 8. IAEA, Vienna. https://www.iaea.org/publications/7382/environmental-consequences-of-the-chernobyl-accident-and-their-remediation-twenty-years-of-experience. (Accessed 27 October 2022).

International Atomic Energy Agency (IAEA), 2019. Environmental Impact Assessment of the Drawdown of the Chernobyl NPP Cooling Pond as a Basis for Its Decommissioning and Remediation, IAEA-TECDOC-1886. IAEA, Vienna. https://www.iaea.org/publications/13595/environmental-impact-assessment-of-the-drawdown-of-the-chernobyl-npp-cooling-pond-as-a-basis-for-its-decommissioning-and-remediation. (Accessed 19 April 2022).

Igarashi, Y., Onda, Y., Smith, J., Obrizan, S., Kirieiev, S., Demianovych, V., Laptev, G., Bugai, D., Lisovyi, H., Konoplev, A., Zheleznyak, M., Wakiyama, Y., Nanba, K., 2020. Simulating dissolved 90Sr concentrations within a small catchment in the Chernobyl exclusion zone using a parametric hydrochemical model. Sci. Rep. 10, 9818. https://doi.org/10.1038/s41598-020-66623-4.

Kanivets, V., Laptev, G., Konoplev, A., Lisovyi, H., Derkach, G., Voitsekhovych, O., 2020. Distribution and dynamics of radionuclides in the Chernobyl cooling pond. In: Konoplev, A., Kato, K., Kalmykov, S. (Eds.), Behavior of Radionuclides in the Environment II. Springer, Singapore, pp. 349–405 https://doi.org/10.1007/978-981-15-3568-0_8.

Kashparov, V., Levchuk, S., Zhurba, M., Protsak, V., Khomutinin, Y., Beresford, N.A., Chaplow, J.S., 2018. Spatial datasets of radionuclide contamination in the Ukrainian Chernobyl exclusion zone. Earth Syst. Sci. Data 10, 339–353. https://doi.org/10.5194/essd-10-339-2018.

Kireev, S.I., Demyanovich, O.V., Smirnova, K.I., Vishnevsky, D.O., Obrizan, S.M., Godun, B.O., Gurin, O.S., Nikitina, S.I., 2013. Radiation situation at the territory of exclusion zone in 2012. Probl. Chernobyl Exclusion Zone 11, 18e37 (in Ukrainian) http://www.chornobyl.net/wp-content/uploads/2018/01/digest-11.zip.

Ledenev, A.I., Ovcharov, P.A., Mishunina, I.B., Antropov, V.M., 1995. Results of complex studies in radiation state of temporary areas for radioactive waste localization in the Chernobyl estrangement zone. Rezul`taty kompleksnykh issledovanij radiatsionnogo sostoyaniya punktov vremennoj lokalizatsii radioaktivnykh otkhodov v Zone otchuzhdeniya ChAEhS." Ukraine, (in Russian) . https://www.osti.gov/etdeweb/biblio/429115. (Accessed 19 January 2022).

Le Gal La Salle, C., Aquilina, L., Fourre, E., Jean-Baptiste, P., Michelot, J.-L., Roux, C., Bugai, D., Labasque, T., Simonucci, C., Van, M.N., Noret, A., Bassot, S., Dapoigny, A., Baumier, D., Verdoux, P., Stammose, D., Lancelot, J., 2012. Groundwater residence time downgradient of Trench No. 22 at the Chernobyl PilotSite: constraints on hydrogeological aquifer functioning. Appl. Geochemistry. 27, 1304–1319. https://doi.org/10.1016/j.apgeochem.2011.12.006.

Lerebours, A., Gudkov, D., Nagorskaya, L., Kaglyan, A., Rizewski, V., Leshchenko, A., Bailey, E.H., Bakir, A., Ovsyanikova, S., Laptev, G., Smith, J.T., 2018. Impact of environmental radiation on the health and reproductive status of fish from Chernobyl. Environ. Sci. Technol. 52, 9442–9450. https://doi.org/10.1021/acs.est.8b02378.

Mappes, T., Boratyński, Z., Kivisaari, K., Lavrinienko, A., Milinevsky, G., Mousseau, T.A., Møller, A.P., Tukalenko, E., Watts, P.C., 2019. Ecological mechanisms can modify radiation effects in a key forest mammal of Chernobyl. Ecosphere 10, e02667. https://doi.org/10.1002/ecs2.2667.

Matoshko, A., Bugai, D., Dewiere, L., Skalskyy, A., 2004. Sedimentological study of the Chernobyl NPP site to schematise radionuclide migration conditions. Environ. Geol. 46, 820–830.. https://doi.org/10.1007/s00254-004-1067-3.

Molitor, N., Thierfeldt, S., Haneke, K., Nitzsche, O., Bugai, D., Sizov, A., Drace, Z., 2017. Recent safety assessment findings on management of legacy wastes from Chornobyl accident. Proc. of the II Int. Conf. on Nuclear Decommissioning and Environment Recovery (INUDECO17), p. 38.

Nasvit, O., 2002. Radioecological situation in the cooling pond of chornobyl NPP. In: Imanaka, T. (Ed.), Recent Research Activities About the Chernobyl NPP Accident in Belarus, Ukraine and Russia. KUR REPORT OF KYOTO UNIVERSITY RESEARCH REACTOR INSTITUTE, Osaka (Japan) , pp. 74–85.. http://www.rri.kyoto-u.ac.jp/PUB/report/04_kr/img/ekr010.pdf. (Accessed 15 June 2022).

Onda, Y., Taniguchi, K., Yoshimura, K., Kato, H., Takahashi, J., Wakiyama, Y., Coppin, F., Smith, H., 2020. Radionuclides from the Fukushima daiichi nuclear power plant in terrestrial systems. Nat. Rev. Earth Environ. 1, 644–660. https://doi.org/10.1038/s43017-020-0099-x.

Onishi, Y., Kivva, S.L., Zheleznyak, M.J., Voitsekhovich, O.V., 2007. Aquatic assessment of the Chernobyl nuclear accident and its remediation. J. Environ. Eng. 113, 1015–1023. https://doi.org/10.1061/(ASCE)0733-9372(2007)133:11(1015).

Roux, C., Le Gal La Salle, C., Simonucci, C., Van, M.N., Fifield, L.K., Diez, Bassot, S., Simler, R., Bugai, D., Kashparov, V., Lancelot, J., 2014. High 36Cl/Cl ratios in Chernobyl groundwater. J. Environ. Radioact. 138, 19–32. https://doi.org/10.1016/j.jenvrad.2014.07.008.

Slater, L.D., Ntarlagiannis, D., Day-Lewis, F.D., Mwakanyamale, K., Versteeg, R.J., Ward, A., Strickland, C., Johnson, C.D., Lane, J.W., 2010. Use of electrical imaging and distributed temperature sensing methods to characterize surface water–groundwater exchange regulating uranium transport at the Hanford 300 Area, Washington. Water Resour. Res. 46, W10533. https://doi.org/10.1029/2010WR009110.

Tyler, S.W., 2020. Are arid regions always that appropriate for waste disposal? examples of complexity from Yucca Mountain, Nevada. Geosciences 10. https://doi.org/10.3390/geosciences10010030.

Van, M.N., Bugai, D., Kashparov, V., 2009. The experimental platform in Chernobyl: an international research polygon in the exclusion zone for soil and groundwater contamination. In: Oughton, D.H., Kashparov, V. (Eds.), Radioactive Particles in the Environment. NATO Science for Peace and Security Series C: Environmental Security. Springer Science & Business Media B.V, Ukraine, pp. 197–208.

Van, M.N., Gaudet, J.P., Phrommavanh, V., Laurent, J.P., Bugai, D., Biron, R., 2012. Flow in the unsaturated zone around a shallow subsurface radioactive waste trench: interpretation of an infiltration–drainage test at the Chernobyl pilot site. Appl. Geochem. 27, 1297–1303. https://doi.org/10.1016/j.apgeochem.2011.08.009.

World Health Organization (WHO), 2017. Guidelines for drinking-water quality: fourth edition incorporating the first addendum. Geneva. https://www.who.int/publications/i/item/9789241549950.

Zachara, J.M., Long, P.E., Bargar, J., Davis, J.A., Fox, P., Fredrickson, J.K., Freshley, M.D., Konopka, A.E., Liu, C., McKinley, J.P., Rockhold, M.L., Williams, K.H., Yabusaki, S.B., 2013. Persistence of uranium groundwater plumes: contrasting mechanisms at two DOE sites in the groundwater–river interaction zone. J. Contam. Hydrol. 147, 45–72. https://doi.org/10.1016/j.jconhyd.2013.02.001.